

Exenatide inhibits NF- κ B and attenuates ER stress in diabetic cardiomyocyte models

Zhenhong Fu¹, David Mui², Hang Zhu¹, Ying Zhang¹

¹Department of Cardiology, The First Medical Center, Chinese PLA General Hospital, Beijing, China

²Perelman School of Medicine, University of Pennsylvania, Philadelphia, PA 19104, USA

Correspondence to: Hang Zhu, Ying Zhang; **email:** zhuhang301@126.com, angelazhang301@163.com

Keywords: ER stress, exenatide, hyperglycemia, NF- κ B signaling pathway, cardiomyocyte

Received: October 15, 2019

Accepted: April 17, 2020

Published: May 11, 2020

Copyright: Fu et al. This is an open-access article distributed under the terms of the Creative Commons Attribution License (CC BY 3.0), which permits unrestricted use, distribution, and reproduction in any medium, provided the original author and source are credited.

ABSTRACT

Exenatide is used to treat patients with type-2 diabetes and it also exerts cardioprotective effects. Here, we tested whether Exenatide attenuates hyperglycemia-related cardiomyocyte damage by inhibiting endoplasmic reticulum (ER) stress and the NF- κ B signaling pathway. Our results demonstrated that hyperglycemia activates the NF- κ B signaling pathway, eliciting ER stress. We also observed cardiomyocyte contractile dysfunction, inflammation, and cell apoptosis induced by hyperglycemia. Exenatide treatment inhibited inflammation, improved cardiomyocyte contractile function, and rescued cardiomyocyte viability. Notably, re-activation of the NF- κ B signaling pathway abolished Exenatide's protective effects on hyperglycemic cardiomyocytes. Taken together, our results demonstrate that Exenatide directly reduces hyperglycemia-induced cardiomyocyte damage by inhibiting ER stress and inactivating the NF- κ B signaling pathway.

INTRODUCTION

Excessive glucose intake is considered an independent risk factor for the development of obesity and diabetes. The primary complications of diabetes or obesity include diabetic cardiomyopathy, neuropathy, hyperglycemia-related kidney damage, retinopathy, and food damage. Among these, cardiovascular complications account for most of diabetes-related deaths [1]. Despite numerous efforts into advancing therapeutic approaches for diabetes, anti-diabetic medications do not seem to prevent the cardiovascular damage induced by diabetes. Recently, Exenatide, a glucagon-like protein-1 receptor agonist, was clinically used to treat patients with type-2 diabetes. While cardioprotective effects have been reported for Exenatide, the underlying molecular mechanisms remain unclear [2, 3].

Protein peroxidation promotes diabetes [4, 5]. Glycosylative, phosphorylative, and oxidative

modifications of cytoplasmic proteins, induced by chronic hyperglycemia, change the normal patterns of protein folding and degradation in cells [6–8]. Additionally, abnormal post-transcriptional modifications correlate with disturbed glucose metabolism. In the cytoplasm, the endoplasmic reticulum (ER) is the main location for protein synthesis, modification, transport and release [9, 10]. Abnormal protein modifications seem to occur in the ER, followed by accumulation of unfolded proteins in the ER lumen. This process is termed “ER stress” and is regulated by PERK, ATF6 and IRE1 [11]. Although ER stress contributes to the development of diabetic cardiomyopathy [12, 13], there is no data explaining Exenatide's effects on ER stress under hyperglycemia stress.

ER stress contributes to cellular inflammation and death through distinct signaling pathways [14, 15]. NF- κ B promotes inflammation by upregulating the transcription of pro-inflammatory factors [16]. In addition, NF- κ B may promote ER stress by

upregulating the transcription and activity of proteins in the JNK pathway [17]. Furthermore, NF- κ B is also a downstream effector of hyperglycemia and increased NF- κ B activity has been noted in hyperglycemia-treated cardiomyocytes [18, 19]. Therefore, this suggests that NF- κ B may promote ER stress induced by hyperglycemia. Accordingly, here we tested the hypothesis that Exenatide attenuates hyperglycemia-related cardiomyocyte damage by inhibiting ER stress and the NF- κ B signaling pathway.

RESULTS

Exenatide improves cardiomyocyte viability and reduces inflammation response induced by hyperglycemia

In this study, hyperglycemia was induced in cardiomyocytes [20], which were then treated with Exenatide. The viability of cardiomyocytes was determined through CCK8 assay. As shown in Figure 1A, cardiomyocyte viability was reduced in response to

hyperglycemia whereas exenatide treatment improved it. In agreement with this effect, we also observed an increase in TUNEL-stained apoptotic cells after hyperglycemia treatment (Figure 1B, 1C). Exenatide treatment reduced the ratio of TUNEL-positive cells, reconfirming that such treatment increases cardiomyocyte viability and survival. In addition to cell death, we also assessed the inflammation response by measuring the levels of pro-inflammatory factors. As shown in Figure 1D, 1E, compared to the control group, MCP1 and TNF α transcription was elevated in hyperglycemic cells. On the other hand, Exenatide treatment inhibited the upregulation of such pro-inflammatory factors, suggesting that Exenatide inhibits hyperglycemia-induced inflammation in cardiomyocytes.

Exenatide treatment enhances the function of hyperglycemia-treated cardiomyocytes

We isolated single cardiomyocytes after hyperglycemia treatment and assessed their contractile properties [21, 22]. As shown in Figure 2A–2D, the peak shortening

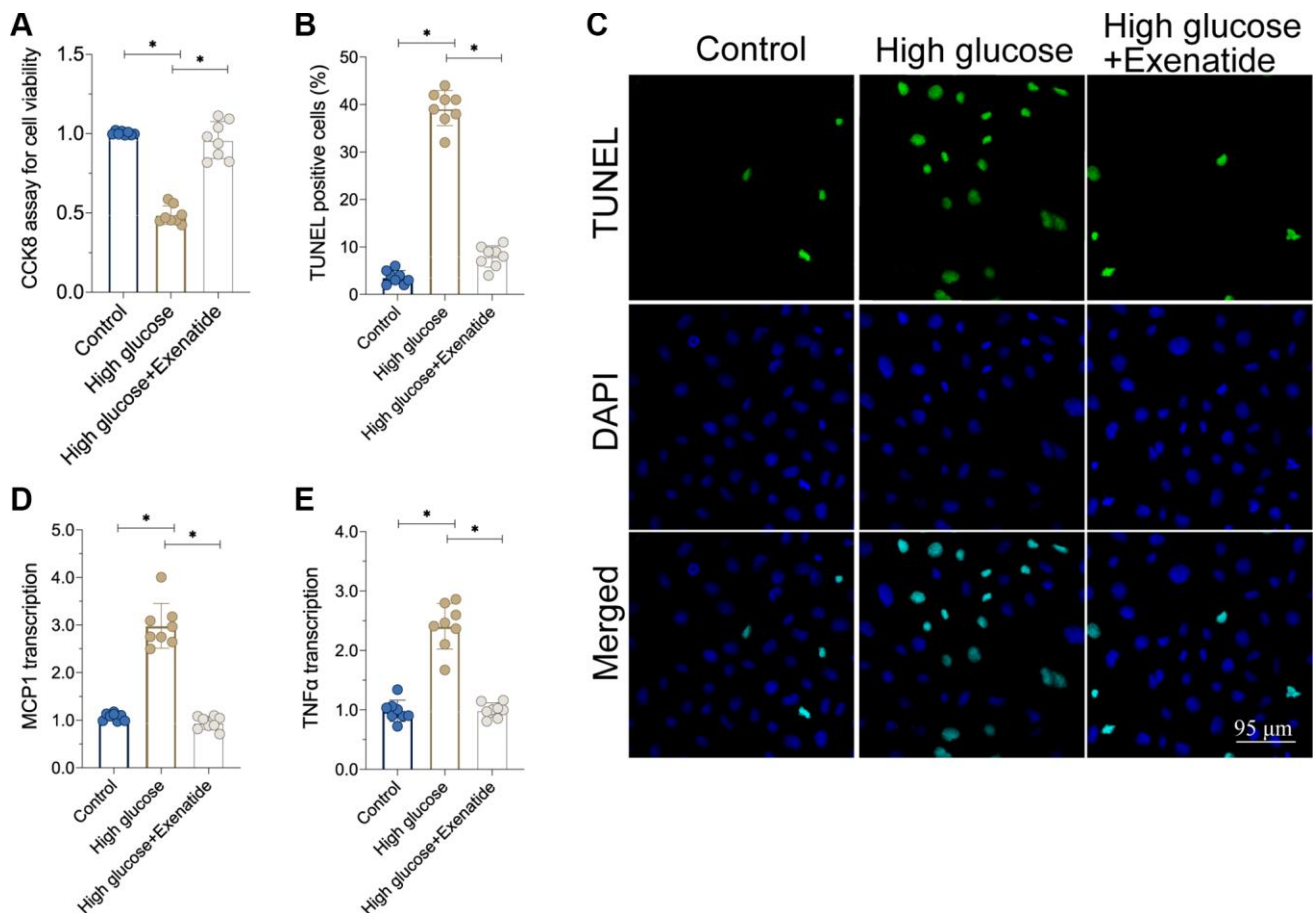


Figure 1. Exenatide attenuates hyperglycemia-induced cell apoptosis and inflammation. (A) CCK8 assay for cell viability. (B, C) TUNEL staining for apoptotic cells. (D, E) qPCR assay for MCP1 and TNF α transcription. *P<0.05.

rate was downregulated in the hyperglycemia group. Similarly, the maximal velocity of shortening ($+dL/dt$) and maximal velocity of re-lengthening ($-dL/dt$) were also impaired by hyperglycemia in cardiomyocytes. The time-to-peak shortening (TPS) was elevated in hyperglycemic cardiomyocytes when compared to controls. Therefore, this indicates that cardiomyocytes contraction and relaxation functions are compromised by hyperglycemia, whereas Exenatide treatment

restored the peak shortening rate, $+dL/dt$, $-dL/dt$ and TPS (Figure 2A–2D). This suggests that cardiomyocyte function could be sustained by Exenatide under hyperglycemic stress. At the molecular level, cardiomyocyte contractility is controlled by cytoskeletal proteins such as Myosin. Interestingly, Myosin levels were reduced in hyperglycemic cardiomyocytes whereas Exenatide treatment increased them, thereby rescuing contractile functions.

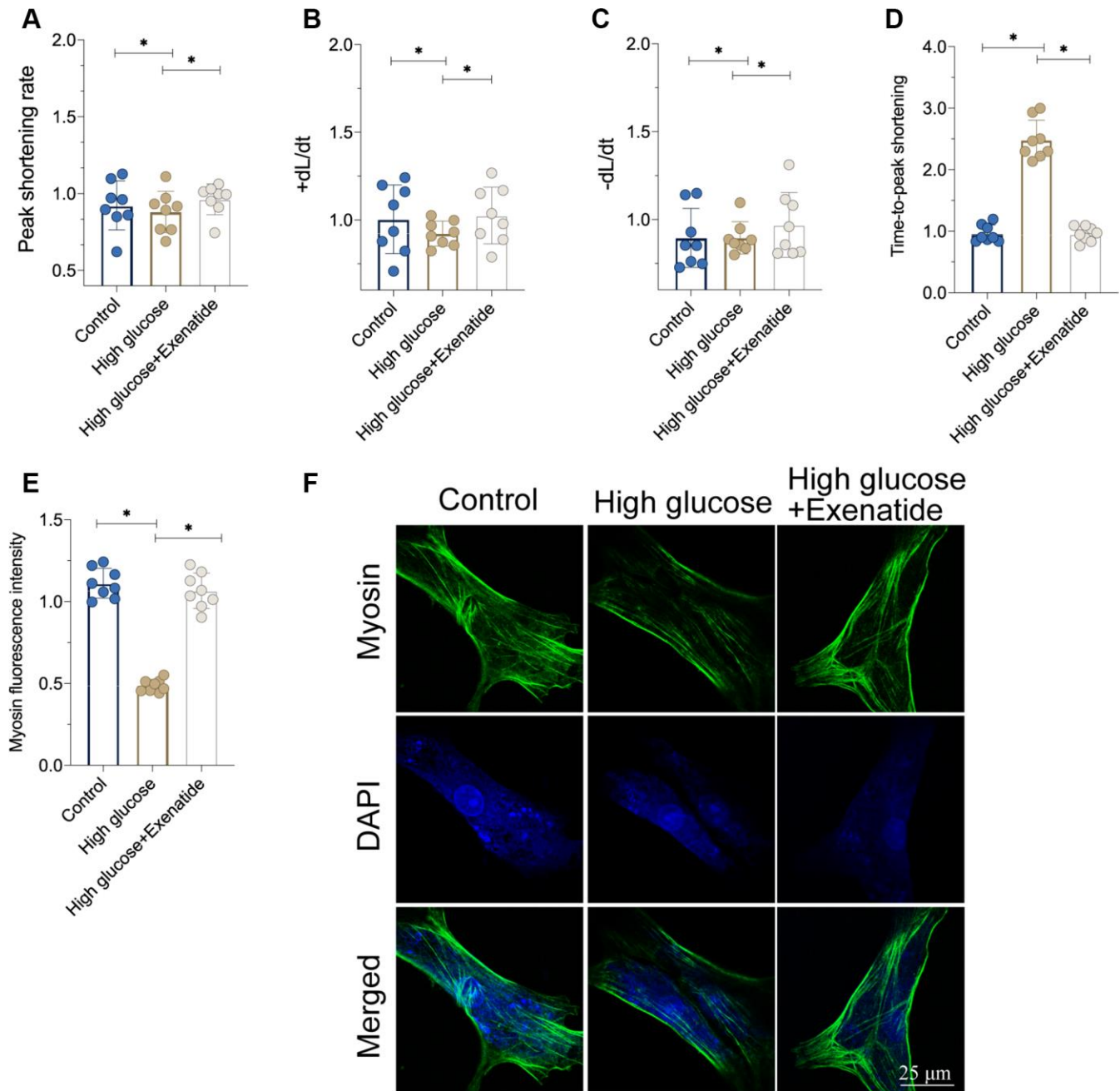


Figure 2. Exenatide treatment improves cardiomyocytes function under hyperglycemia stress. (A–D) Signal of cardiomyocyte contractile parameters measured in response to Exenatide treatment. (E, F) Myosin expression determined through immunofluorescence. * $P < 0.05$.

Exenatide inhibits ER stress and the NF-κB signaling pathway

As discussed above, hyperglycemia-induced cardiomyocyte damage is associated with ER stress and NF-κB signaling pathway activation [23, 24]. Accordingly, we observed alterations in ER stress and NF-κB activation in response to Exenatide treatment. As shown in Figure 3A–3C, the transcriptions of PERK, ATF6 and IRE1 were increased in response to hyperglycemia treatment, suggesting an activation of ER stress. In addition, we also found that the activity of

NF-κB was also augmented in hyperglycemic cells (Figure 3D). Interestingly, Exenatide treatment reduced the levels of PERK, ATF6 and IRE1 (Figure 3A–3C), suggesting that Exenatide inhibits ER stress. In addition, NF-κB activity was also inhibited by Exenatide treatment (Figure 3D). We also observed an upregulation in NF-κB expression in hyperglycemic cells through immunofluorescence assays while Exenatide treatment reduced NF-κB expression to near-normal levels (Figure 3E, 3F). Overall, our results indicate that Exenatide regulates inhibits ER stress and the NF-κB signaling pathway.

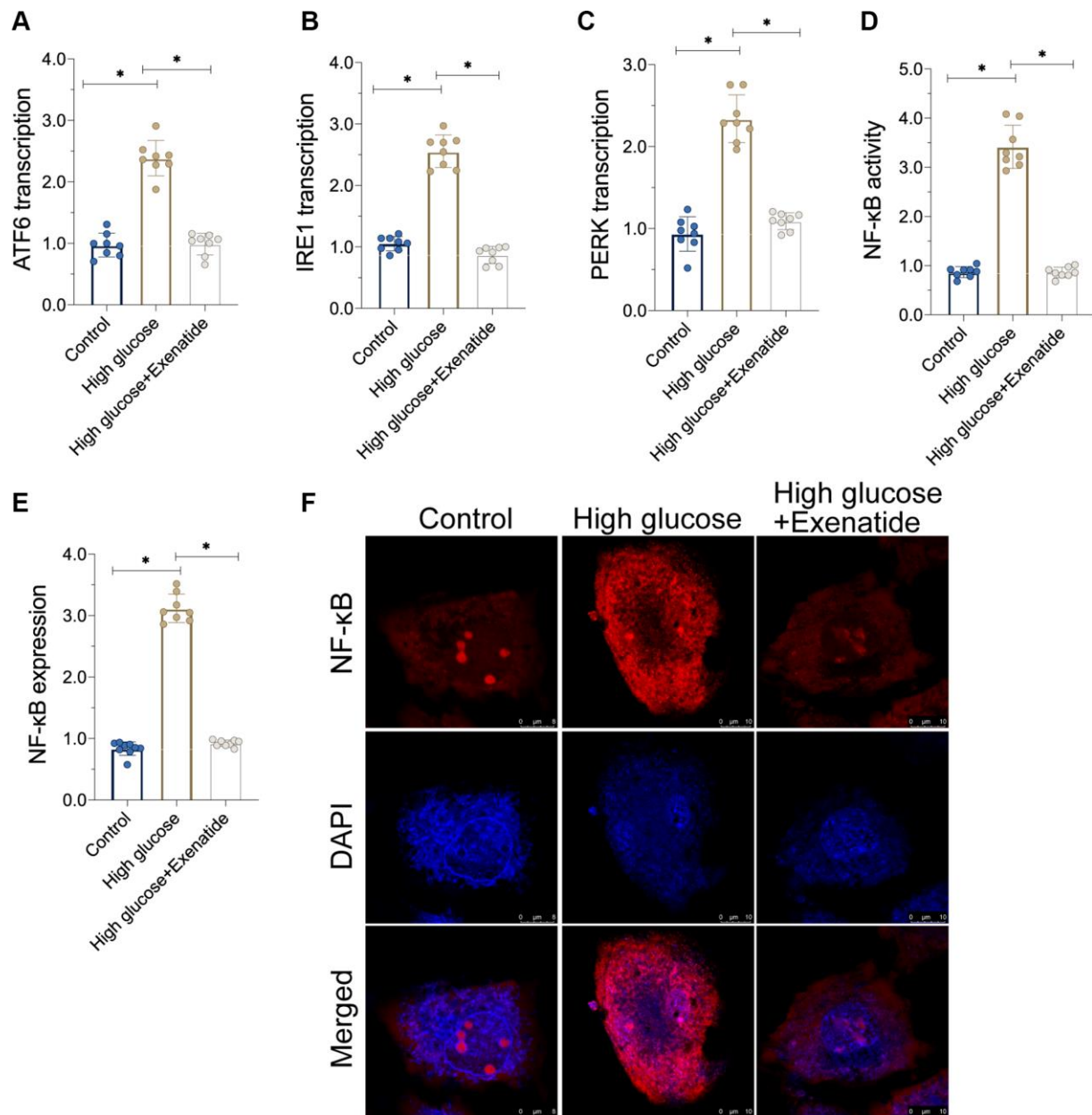


Figure 3. Exenatide reduces ER stress and the activation of NF-κB signaling pathway. (A–C) qPCR assay for ATF6, IRE1 and PERK transcription. (D) ELISA assay for NF-κB activity. (E–F) Immunofluorescence staining for NF-κB. *P<0.05.

Re-activation of the NF- κ B pathway abolishes Exenatide-mediated ER stress inhibition

To verify whether NF- κ B pathway is required for Exenatide-induced ER stress protection [25], we added an agonist, Betulinic acid (BA), to activate the NF- κ B pathway. Then, ER stress was analyzed again. As shown in Figure 4A–4C, ER stress markers were elevated in the hyperglycemia group compared to controls. Exenatide treatment prevented the upregulation of ER stress-related markers whereas these

effects were not evident in BA-treated cardiomyocytes. Thus, our results indicate that inhibition of the NF- κ B pathway by Exenatide is required for ER stress inhibition. Additionally, we also measured the activity of caspase-12 and CHOP. As shown in Figure 4D–4F, we observed increased caspase-12 and CHOP activity in the hyperglycemia group. Although Exenatide treatment inhibited caspase-12 and CHOP activity, this action is not apparent in BA-treated cardiomyocytes. Altogether, our results confirm that Exenatide inhibits ER stress through the NF- κ B pathway.

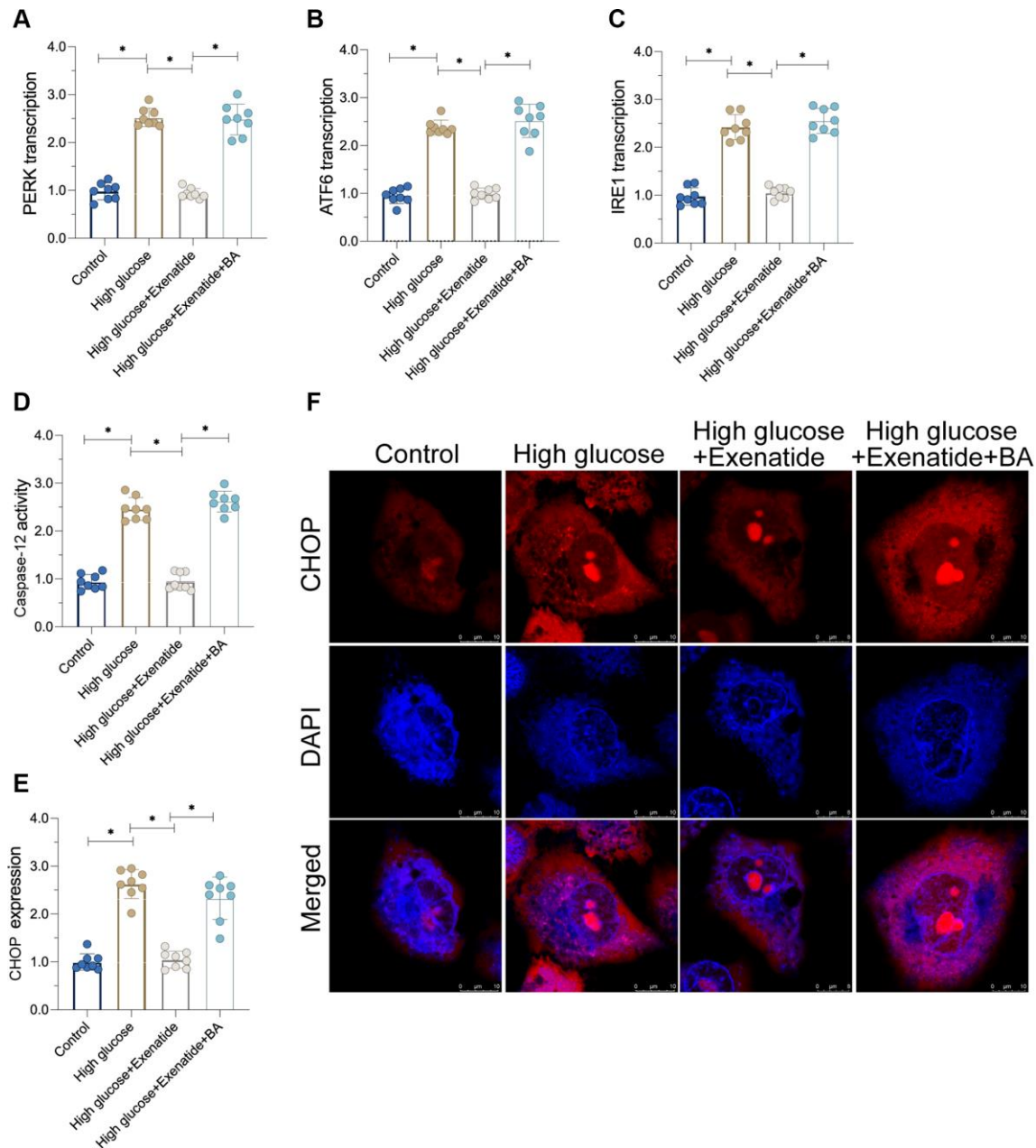


Figure 4. Re-activation of NF- κ B promotes cardiomyocyte damage. (A–C) qPCR assay for ATF6, IRE1 and PERK transcription in the presence of BA to activate NF- κ B. (D) ELISA assay for caspase-12 activity. (E, F) Immunofluorescence staining for CHOP. *P<0.05.

Re-activation of the NF- κ B pathway promotes cardiomyocyte inflammation and death

Next, we sought to determine whether the NF- κ B pathway is involved in Exenatide-regulated cardiomyocyte death and inflammation [26]. First, cardiomyocyte viability, as evaluated through CCK8 assay, was reduced after exposure to hyperglycemia treatment whereas Exenatide treatment restored cardiomyocyte viability in a NF- κ B-dependent manner. Indeed, re-activation of the NF- κ B pathway abolished the pro-survival effects of Exenatide on cardiomyocytes (Figure 5A). In addition to CCK8 assay, we also measured the activity of caspase-3, a critical regulator of cell apoptosis. As shown in Figure 5B, caspase-3 activity was increased in the hyperglycemia group. Exenatide caused a decrease in caspase-3 activity whereas re-activation of the NF- κ B pathway through supplementation with BA induced an activation of caspase-3 in Exenatide-treated cardiomyocytes. Overall, our results verified that NF- κ B pathway inhibition accounts for Exenatide-mediated cardiomyocyte survival. In addition to cardiomyocyte viability, we also evaluated the inflammation response. Pro-inflammatory factors were upregulated in response to hyperglycemia treatment whereas Exenatide treatment inhibited the transcription of inflammatory factors (Figure 5C, 5D). Re-activation of the NF- κ B pathway abolished Exenatide-mediated inflammation inhibition. Therefore, our data suggest that Exenatide also promotes cardiomyocyte viability and inhibits inflammation through the NF- κ B pathway.

DISCUSSION

Diabetic cardiomyopathy is caused by chronic hyperglycemia stress. Cardiomyocyte apoptosis and microvascular damage are the primary factors promoting the development of diabetic cardiomyopathy [27]. The clinical features of diabetic cardiomyopathy include decreased cardiac output and limited cardiac relaxation. Additionally, cardiovascular disorders are the most dangerous complication for diabetic patients [28, 29]. More than 40% of patients with type-2 diabetes will suffer from cardiovascular complications and more than half of those will die from diabetic cardiomyopathy. Although insulin administration can treat type-2 diabetes, its chronic use increases the risk of cancer. Furthermore, most patients often present hypoglycemia after insulin treatment, with no beneficial effects on diabetes-related cardiovascular complications.

Exenatide is a recently developed drug to treat diabetes [30, 31]. The molecular mechanisms underlying Exenatide's functions involve GLP-1 receptor

activation, which promotes glucose utilization. Exenatide elicits only a low hypoglycemic response and cardiovascular benefits increase with extended use of the drug [32]. In this study, we investigated the mechanisms underlying Exenatide-mediated cardio-protection *in vitro*.

ER stress entails a series of protein modification and folding/unfolding events in response to abnormal quantities and decreased quality of proteins in the ER lumen [13, 33]. Although proteins are primarily translated from mRNA by ribosomes, the functional configurations and post-transcriptional modifications of many proteins are attained in the ER [34, 35]. After chronic hyperglycemia, the levels of glucose in the cytoplasm are high, contributing to protein degradation and oxidation. Therefore, ER stress is followed by abnormal protein accumulation [36, 37]. Our data here indicated that hyperglycemia treatment triggered ER stress, followed by cardiomyocyte dysfunction and

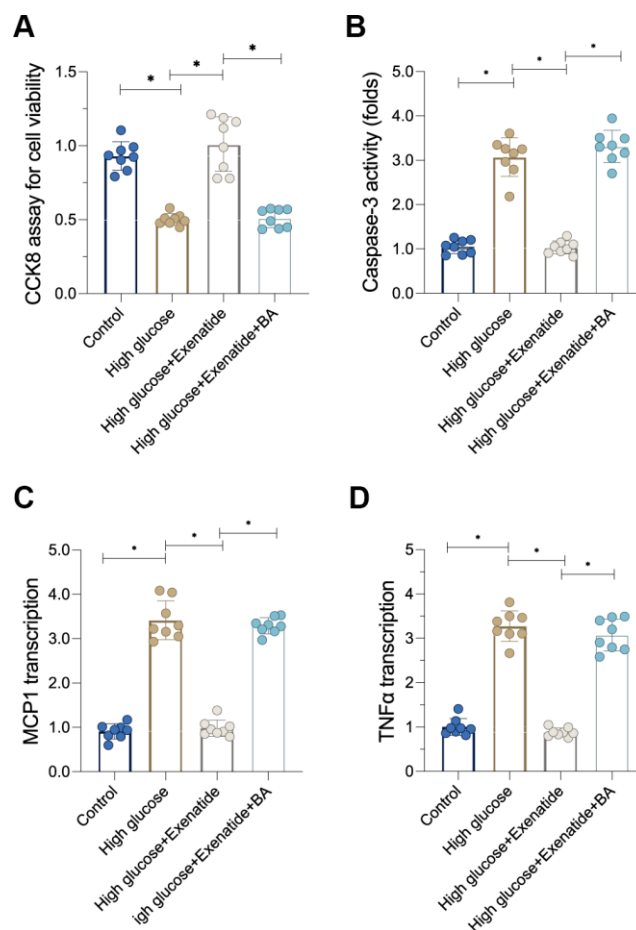


Figure 5. Re-activation of NF- κ B induces cardiomyocyte death and inflammation. (A) CCK8 assay for cell viability. (B) ELISA assay for caspase-3 activity. (C, D) qPCR assay for MCP1 and TNF α transcription. *P<0.05.

death. Interestingly, Exenatide treatment attenuated ER stress, thereby sustaining cardiomyocyte contractile functions and favoring cardiomyocyte survival [38, 39]. These results identified ER stress as a downstream target of Exenatide treatment. Indeed, protection of the ER against abnormal protein modifications promotes cardiomyocyte viability [40, 41].

In our study, we found that inflammation and ER stress were under the control of the NF- κ B pathway. In contrast, hyperglycemia-activated NF- κ B was inhibited by Exenatide. These results demonstrate that Exenatide exerts protective effects on cardiomyocytes through the NF- κ B signaling pathway, in agreement with previous studies [42, 43]. Indeed, such studies have shown that inhibition of NF- κ B prevents heart inflammation [44, 45] while improving oxidative stress and countering the downregulation of anti-oxidative factors [46, 47]. In addition, myocardial damage induced by a high-fat diet was also normalized by NF- κ B inhibition [48]. The pro-inflammatory role of NF- κ B in cardiomyocyte damage has also been observed in myocardial ischemia-reperfusion injury [49, 50].

While our observations will need to be validated in clinical settings, our results here demonstrated that Exenatide treatment inhibited inflammation and oxidative stress and improved viability in cardiomyocytes during hyperglycemia stress. Specifically, Exenatide inhibited the NF- κ B pathway and attenuated ER stress, supporting cardiomyocyte survival. These findings highlight NF- κ B as a potential therapeutic target in the treatment of diabetes-induced cardiomyopathies.

MATERIALS AND METHODS

Cell culture

We cultured H9C2 cells, as previously described [51]. Hyperglycemia stimulation was mimicked as previously reported [52]. In brief, H9C2 cells were cultivated in DMEM medium supplemented with EGF Single Quots (PELOBiotech GmbH, Martinsried, Germany) plus 10% FBS and used until passage five. Hyperglycemia stress was induced by incubating the cells in 25 mmol/L high glucose medium for 12 h. The cells were treated with exenatide (10 μ M) and incubated for 12 h before high-glucose treatment. Betulinic acid (BA) at 5 nM was added to activate the NF- κ B signaling pathway [53].

Immunoblotting

Proteins were extracted from cell lysates (McA or primary mouse hepatocytes) and tissue lysates (liver) in RIPA buffer (50 mM Tris pH 7.4, 150 mM NaCl,

0.25% sodium deoxycholate, 1% Nonidet P-40) [54]. Total protein amounts were quantified using Bio-Rad DC assay kit (Bio-Rad, Hercules, CA). In general, 20–80 μ g of protein homogenate were separated by SDS-PAGE and subsequently electroblotted onto PVDF membranes (Bio-Rad). Membranes were blocked with fat-free milk powder (5% w/v) dissolved in Tris-buffered saline (15 mM NaCl and 10 mM Tris/HCl, pH 7.5) containing 0.01% Tween 100 (TBS-T), washed, and incubated overnight at 4 °C with the appropriate primary antibody (see above) [55]. Infrared fluorescent-labeled secondary antibodies were prepared at 1:15,000 dilution in TBS-T with 5% fat-free milk powder and incubated for 1 h at room temperature. Protein band quantification was performed using ImageJ (NIH, Bethesda, MD) [56].

Immunofluorescence and confocal microscopy

Cells were grown on fibronectin-coated glass coverslips. After administering the corresponding treatments, the media were removed and cell monolayers were washed with ice-cold PBS. The cells were then fixed with 7.5% of neutral-buffered formalin solution containing 0.025% of glutaraldehyde for 10 min at room temperature [57]. The specimens were then washed and permeabilized with PBS containing 0.1% Triton (PBS-T) or 0.1% digitonin, and blocked for 1 h with PBS supplemented with 5% bovine serum albumin and 2% goat serum (Sigma) [58]. Afterwards, specimens were incubated overnight in blocking buffer containing the corresponding primary antibodies at a 1:200 concentration. Specimens were washed and incubated for 1 h at room temperature with the corresponding secondary antibodies (see above) at a 1:400 dilution in blocking buffer. Secondary antibodies conjugated to Alexa fluorophores were purchased from Molecular Probes (Life Technologies). DAPI was used to stain nuclei [59]. For some co-localization experiments, when two primary antibodies were raised in rabbits, one of the primary antibodies was detected using the regular procedure, while the second primary antibody was conjugated with Alexa fluorophore 488 using a commercially available kit (Life Technologies) [60]. Confocal images were acquired with a Leica TCS SP5 II confocal microscope by using a 405 diode laser (excitation 405 nm), a multiline argon laser (excitation 488 nm), and two HeNe lasers (excitation 543 and 633 nm) with a 40 \times Apochromat, numerical aperture 1.25 – Oil objective and with a 63 \times Apochromat, numerical aperture 1.40- Oil objective [1].

RNA isolation and Quantitative Real Time (QRT)-PCR analysis

RNA was isolated from cultured cells using TRIzol Reagent following the manufacturer's instructions (Life

Technologies) [61, 62]. Two μg of total RNA were reverse-transcribed to cDNA using the Verso cDNA Synthesis kit (ThermoFisher Scientific). QRT-PCR was carried out with TaqMan chemistry and probes (Applied Biosystems). Gene expression analyses were performed with the ABI Step One Plus QRT-PCR machine (Applied Biosystems) [63].

Mitochondrial membrane potential assay

Mitochondrial membrane potential in cells was measured by JC-1 fluorescence intensity. In brief, cells were plated at 50,000 cells/well in a 96-well black bottom dish. After hyperglycemia stimulation, cells were incubated with 10 μM JC-1 and DAPI for 30 min in the dark [64]. Then, JC-1 and Hoechst (360/450) fluorescence intensity was measured using a SpectraMax3 plate reader (Molecular devices, Sunnyvale, California). The JC-1/DAPI fluorescence ratio is used to determine the mitochondrial membrane potential [65].

Oxidative stress and superoxide production

Mitochondrial ROS production was measured with a fluorometric assay, as described [66]. Activity of aconitase was measured in isolated mitochondria using a spectrophotometric assay, and tissue ROS levels were measured by the conversion of nonfluorescent 2',7'-dichlorofluorescein-diacetate (DCFDA) to the highly fluorescent 2',7'-dichlorofluorescein (DCF), as described before. In cells, ROS levels were measured by CellRox reagent in accordance with the manufacturer's instructions (Thermo Fisher Scientific, Waltham, MA) [67].

Statistical analysis

All experiments were conducted in at least triplicate. Data are expressed as the mean \pm SEM. Statistical differences were analyzed using GraphPad Prism software (GraphPad Software Inc., San Diego, CA). We tested for normality in the distribution of the sample groups using the D'Agostino-Pearson omnibus and the Shapiro-Wilk normality tests [68]. Statistical significance was then determined by unpaired two-tailed Student's *t*-test with a threshold of significance set at $p < 0.05$.

CONFLICTS OF INTEREST

The authors declare that they have no conflicts of interest.

FUNDING

This study was supported by National Natural Science Foundation of China (funding number 81500269) and

Open project of National Geriatrics Clinical Medicine Research Center (funding number NCRCG-PLAGH-2019002).

The affiliation of the second funding belongs to National Clinical Research Center of Geriatrics Disease, Beijing, China.

REFERENCES

1. Zhang HF, Wang YL, Tan YZ, Wang HJ, Tao P, Zhou P. Enhancement of cardiac lymphangiogenesis by transplantation of CD34⁺VEGFR-3⁺ endothelial progenitor cells and sustained release of VEGF-C. *Basic Res Cardiol*. 2019; 114:43. <https://doi.org/10.1007/s00395-019-0752-z> PMID:[31587086](https://pubmed.ncbi.nlm.nih.gov/31587086/)
2. Yellon DM, He Z, Khambata R, Ahluwalia A, Davidson SM. The GTN patch: a simple and effective new approach to cardioprotection? *Basic Res Cardiol*. 2018; 113:20. <https://doi.org/10.1007/s00395-018-0681-2> PMID:[29666943](https://pubmed.ncbi.nlm.nih.gov/29666943/)
3. Birnbaum Y, Tran D, Bajaj M, Ye Y. DPP-4 inhibition by linagliptin prevents cardiac dysfunction and inflammation by targeting the Nlrp3/ASC inflammasome. *Basic Res Cardiol*. 2019; 114:35. <https://doi.org/10.1007/s00395-019-0743-0> PMID:[31388770](https://pubmed.ncbi.nlm.nih.gov/31388770/)
4. Wiedmann F, Schulte JS, Gomes B, Zafeiriou MP, Ratte A, Rathjens F, Fehrmann E, Scholz B, Voigt N, Müller FU, Thomas D, Katus HA, Schmidt C. Atrial fibrillation and heart failure-associated remodeling of two-pore-domain potassium (K_{2P}) channels in murine disease models: focus on TASK-1. *Basic Res Cardiol*. 2018; 113:27. <https://doi.org/10.1007/s00395-018-0687-9> PMID:[29881975](https://pubmed.ncbi.nlm.nih.gov/29881975/)
5. Rong B, Feng R, Liu C, Wu Q, Sun C. Reduced delivery of epididymal adipocyte-derived exosomal resistin is essential for melatonin ameliorating hepatic steatosis in mice. *J Pineal Res*. 2019; 66:e12561. <https://doi.org/10.1111/jpi.12561> PMID:[30659651](https://pubmed.ncbi.nlm.nih.gov/30659651/)
6. Boga JA, Caballero B, Potes Y, Perez-Martinez Z, Reiter RJ, Vega-Naredo I, Coto-Montes A. Therapeutic potential of melatonin related to its role as an autophagy regulator: A review. *J Pineal Res*. 2019; 66:e12534. <https://doi.org/10.1111/jpi.12534> PMID:[30329173](https://pubmed.ncbi.nlm.nih.gov/30329173/)
7. Madreiter-Sokolowski CT, Waldeck-Weiermair M, Bourguignon MP, Villeneuve N, Gottschalk B, Klec C, Stryeck S, Radulovic S, Parichatikanond W, Frank S,

- Madl T, Malli R, Graier WF. Enhanced inter-compartmental Ca²⁺ flux modulates mitochondrial metabolism and apoptotic threshold during aging. *Redox Biol.* 2019; 20:458–66.
<https://doi.org/10.1016/j.redox.2018.11.003>
PMID:30458321
8. Zhao XM, Wang N, Hao HS, Li CY, Zhao YH, Yan CL, Wang HY, Du WH, Wang D, Liu Y, Pang YW, Zhu HB. Melatonin improves the fertilization capacity and developmental ability of bovine oocytes by regulating cytoplasmic maturation events. *J Pineal Res.* 2018; 64:64.
<https://doi.org/10.1111/jpi.12445>
PMID:28833478
9. Pozzer D, Varone E, Chernorudskiy A, Schiarea S, Missiroli S, Giorgi C, Pinton P, Canato M, Germinario E, Nogara L, Blaauw B, Zito E. A maladaptive ER stress response triggers dysfunction in highly active muscles of mice with SELENON loss. *Redox Biol.* 2019; 20:354–66.
<https://doi.org/10.1016/j.redox.2018.10.017>
PMID:30391828
10. Park HJ, Park JY, Kim JW, Yang SG, Jung JM, Kim MJ, Kang MJ, Cho YH, Wee G, Yang HY, Song BS, Kim SU, Koo DB. Melatonin improves the meiotic maturation of porcine oocytes by reducing endoplasmic reticulum stress during in vitro maturation. *J Pineal Res.* 2018; 64:64.
<https://doi.org/10.1111/jpi.12458>
PMID:29149522
11. Wu X, Zhang L, Miao Y, Yang J, Wang X, Wang CC, Feng J, Wang L. Homocysteine causes vascular endothelial dysfunction by disrupting endoplasmic reticulum redox homeostasis. *Redox Biol.* 2019; 20:46–59.
<https://doi.org/10.1016/j.redox.2018.09.021>
PMID:30292945
12. Shakeri A, Zirak MR, Wallace Hayes A, Reiter R, Karimi G. Curcumin and its analogues protect from endoplasmic reticulum stress: mechanisms and pathways. *Pharmacol Res.* 2019; 146:104335.
<https://doi.org/10.1016/j.phrs.2019.104335>
PMID:31265891
13. Zito E. Targeting ER stress/ER stress response in myopathies. *Redox Biol.* 2019; 26:101232.
<https://doi.org/10.1016/j.redox.2019.101232>
PMID:31181458
14. Wider J, Undyala VV, Whittaker P, Woods J, Chen X, Przyklenk K. Remote ischemic preconditioning fails to reduce infarct size in the Zucker fatty rat model of type-2 diabetes: role of defective humoral communication. *Basic Res Cardiol.* 2018; 113:16.
<https://doi.org/10.1007/s00395-018-0674-1>
PMID:29524006
15. Podaru MN, Fields L, Kainuma S, Ichihara Y, Hussain M, Ito T, Kobayashi K, Mathur A, D'Acquisto F, Lewis-McDougall F, Suzuki K. Reparative macrophage transplantation for myocardial repair: a refinement of bone marrow mononuclear cell-based therapy. *Basic Res Cardiol.* 2019; 114:34.
<https://doi.org/10.1007/s00395-019-0742-1>
PMID:31372765
16. Li DJ, Tong J, Li YH, Meng HB, Ji QX, Zhang GY, Zhu JH, Zhang WJ, Zeng FY, Huang G, Hua X, Shen FM, Wang P. Melatonin safeguards against fatty liver by antagonizing TRAFs-mediated ASK1 deubiquitination and stabilization in a β -arrestin-1 dependent manner. *J Pineal Res.* 2019; 67:e12611.
<https://doi.org/10.1111/jpi.12611>
PMID:31541591
17. Vico TA, Marchini T, Ginart S, Lorenzetti MA, Adán Areán JS, Calabró V, Garcés M, Ferrero MC, Mazo T, D'Annunzio V, Gelpi RJ, Corach D, Evelson P, et al. Mitochondrial bioenergetics links inflammation and cardiac contractility in endotoxemia. *Basic Res Cardiol.* 2019; 114:38.
<https://doi.org/10.1007/s00395-019-0745-y>
PMID:31428876
18. Omidkhoda N, Wallace Hayes A, Reiter RJ, Karimi G. The role of MicroRNAs on endoplasmic reticulum stress in myocardial ischemia and cardiac hypertrophy. *Pharmacol Res.* 2019; 150:104516.
<https://doi.org/10.1016/j.phrs.2019.104516>
PMID:31698066
19. Ettcheto M, Cano A, Busquets O, Manzine PR, Sánchez-López E, Castro-Torres RD, Beas-Zarate C, Verdaguer E, García ML, Olloquequi J, Auladell C, Folch J, Camins A. A metabolic perspective of late onset Alzheimer's disease. *Pharmacol Res.* 2019; 145:104255.
<https://doi.org/10.1016/j.phrs.2019.104255>
PMID:31075308
20. Lee K, Hwang OJ, Reiter RJ, Back K. Flavonoids inhibit both rice and sheep serotonin N-acetyltransferases and reduce melatonin levels in plants. *J Pineal Res.* 2018; 65:e12512.
<https://doi.org/10.1111/jpi.12512> PMID:29851162
21. Kazakov A, Hall RA, Werner C, Meier T, Trouvain A, Rodionycheva S, Nickel A, Lammert F, Maack C, Böhm M, Laufs U. Raf kinase inhibitor protein mediates myocardial fibrosis under conditions of enhanced myocardial oxidative stress. *Basic Res Cardiol.* 2018; 113:42.
<https://doi.org/10.1007/s00395-018-0700-3>
PMID:30191336
22. Jain R, Mintern JD, Tan I, Dewson G, Strasser A, Gray DH. How do thymic epithelial cells die? *Cell Death Differ.* 2018; 25:1002–04.

- <https://doi.org/10.1038/s41418-018-0093-8>
PMID:[29549302](https://pubmed.ncbi.nlm.nih.gov/29549302/)
23. Karwi QG, Bice JS, Baxter GF. Pre- and postconditioning the heart with hydrogen sulfide (H₂S) against ischemia/reperfusion injury in vivo: a systematic review and meta-analysis. *Basic Res Cardiol*. 2017; 113:6.
<https://doi.org/10.1007/s00395-017-0664-8>
PMID:[29242986](https://pubmed.ncbi.nlm.nih.gov/29242986/)
24. Kim S, Jin H, Seo HR, Lee HJ, Lee YS. Regulating BRCA1 protein stability by cathepsin S-mediated ubiquitin degradation. *Cell Death Differ*. 2019; 26:812–25.
<https://doi.org/10.1038/s41418-018-0153-0>
PMID:[30006610](https://pubmed.ncbi.nlm.nih.gov/30006610/)
25. Serocki M, Bartoszevska S, Janaszak-Jasiecka A, Ochocka RJ, Collawn JF, Bartoszewski R. miRNAs regulate the HIF switch during hypoxia: a novel therapeutic target. *Angiogenesis*. 2018; 21:183–202.
<https://doi.org/10.1007/s10456-018-9600-2>
PMID:[29383635](https://pubmed.ncbi.nlm.nih.gov/29383635/)
26. Tatullo M, Makeeva I, Rengo S, Rengo C, Spagnuolo G, Codispoti B. Small molecule GSK-3 antagonists play a pivotal role in reducing the local inflammatory response, in promoting resident stem cell activation and in improving tissue repairing in regenerative dentistry. *Histol Histopathol*. 2019; 34:1195–203.
<https://doi.org/10.14670/HH-18-133> PMID:[31169298](https://pubmed.ncbi.nlm.nih.gov/31169298/)
27. Zhou H, Li N, Yuan Y, Jin YG, Guo H, Deng W, Tang QZ. Activating transcription factor 3 in cardiovascular diseases: a potential therapeutic target. *Basic Res Cardiol*. 2018; 113:37.
<https://doi.org/10.1007/s00395-018-0698-6>
PMID:[30094473](https://pubmed.ncbi.nlm.nih.gov/30094473/)
28. Hofbauer TM, Mangold A, Scherz T, Seidl V, Panzenböck A, Ondracek AS, Müller J, Schneider M, Binder T, Hell L, Lang IM. Neutrophil extracellular traps and fibrocytes in ST-segment elevation myocardial infarction. *Basic Res Cardiol*. 2019; 114:33.
<https://doi.org/10.1007/s00395-019-0740-3>
PMID:[31312919](https://pubmed.ncbi.nlm.nih.gov/31312919/)
29. Hernandez SL, Nelson M, Sampedro GR, Bagrodia N, Defnet AM, Lec B, Emolo J, Kirschner R, Wu L, Biermann H, Shen S, Bubeck Wardenburg J, Kandel JJ. Staphylococcus aureus alpha toxin activates Notch in vascular cells. *Angiogenesis*. 2019; 22:197–209.
<https://doi.org/10.1007/s10456-018-9650-5>
PMID:[30324336](https://pubmed.ncbi.nlm.nih.gov/30324336/)
30. Battelli MG, Bortolotti M, Polito L, Bolognesi A. Metabolic syndrome and cancer risk: the role of xanthine oxidoreductase. *Redox Biol*. 2019; 21:101070.
<https://doi.org/10.1016/j.redox.2018.101070>
PMID:[30576922](https://pubmed.ncbi.nlm.nih.gov/30576922/)
31. Li S, Xu HX, Wu CT, Wang WQ, Jin W, Gao HL, Li H, Zhang SR, Xu JZ, Qi ZH, Ni QX, Yu XJ, Liu L. Angiogenesis in pancreatic cancer: current research status and clinical implications. *Angiogenesis*. 2019; 22:15–36.
<https://doi.org/10.1007/s10456-018-9645-2>
PMID:[30168025](https://pubmed.ncbi.nlm.nih.gov/30168025/)
32. Sasaki N, Itakura Y, Gomi F, Hirano K, Toyoda M, Ishiwata T. Comparison of functional glycans between cancer stem cells and normal stem cells. *Histol Histopathol*. 2019; 34:995–1007.
<https://doi.org/10.14670/HH-18-119>
PMID:[31025698](https://pubmed.ncbi.nlm.nih.gov/31025698/)
33. Liu H, Wang L, Weng X, Chen H, Du Y, Diao C, Chen Z, Liu X. Inhibition of Brd4 alleviates renal ischemia/reperfusion injury-induced apoptosis and endoplasmic reticulum stress by blocking FoxO4-mediated oxidative stress. *Redox Biol*. 2019; 24:101195.
<https://doi.org/10.1016/j.redox.2019.101195>
PMID:[31004990](https://pubmed.ncbi.nlm.nih.gov/31004990/)
34. Trindade F, Vitorino R, Leite-Moreira A, Falcão-Pires I. Pericardial fluid: an underrated molecular library of heart conditions and a potential vehicle for cardiac therapy. *Basic Res Cardiol*. 2019; 114:10.
<https://doi.org/10.1007/s00395-019-0716-3>
PMID:[30659359](https://pubmed.ncbi.nlm.nih.gov/30659359/)
35. Manevitz-Mendelson E, Lechner GS, Barel O, Davidi-Avrahami I, Ziv-Strasser L, Eyal E, Pessach I, Rimon U, Barzilai A, Hirshberg A, Chechekes K, Amariglio N, Rechavi G, et al. Somatic NRAS mutation in patient with generalized lymphatic anomaly. *Angiogenesis*. 2018; 21:287–98.
<https://doi.org/10.1007/s10456-018-9595-8>
PMID:[29397482](https://pubmed.ncbi.nlm.nih.gov/29397482/)
36. Varone E, Pozzer D, Di Modica S, Chernorudskiy A, Nogara L, Baraldo M, Cinquanta M, Fumagalli S, Villar-Quiles RN, De Simoni MG, Blaauw B, Ferreiro A, Zito E. SELENON (SEPN1) protects skeletal muscle from saturated fatty acid-induced ER stress and insulin resistance. *Redox Biol*. 2019; 24:101176.
<https://doi.org/10.1016/j.redox.2019.101176>
PMID:[30921636](https://pubmed.ncbi.nlm.nih.gov/30921636/)
37. Chen X, Chen X, Zhang X, Wang L, Cao P, Rajamanickam V, Wu C, Zhou H, Cai Y, Liang G, Wang Y. Curcuminoid B63 induces ROS-mediated paraptosis-like cell death by targeting TrxR1 in gastric cells. *Redox Biol*. 2019; 21:101061.
<https://doi.org/10.1016/j.redox.2018.11.019>
PMID:[30590310](https://pubmed.ncbi.nlm.nih.gov/30590310/)
38. Zhang Z, Zhang L, Zhou L, Lei Y, Zhang Y, Huang C. Redox signaling and unfolded protein response coordinate cell fate decisions under ER stress. *Redox Biol*. 2019; 25:101047.

- <https://doi.org/10.1016/j.redox.2018.11.005>
PMID:[30470534](https://pubmed.ncbi.nlm.nih.gov/30470534/)
39. Montoya-Zegarra JA, Russo E, Runge P, Jadhav M, Willrodt AH, Stoma S, Nørrelykke SF, Detmar M, Halin C. AutoTube: a novel software for the automated morphometric analysis of vascular networks in tissues. *Angiogenesis*. 2019; 22:223–36.
<https://doi.org/10.1007/s10456-018-9652-3>
PMID:[30370470](https://pubmed.ncbi.nlm.nih.gov/30370470/)
40. Trieb M, Kornej J, Knuplez E, Hindricks G, Thiele H, Sommer P, Scharnagl H, Dargès N, Dinov B, Bollmann A, Husser D, Marsche G, Buettner P. Atrial fibrillation is associated with alterations in HDL function, metabolism, and particle number. *Basic Res Cardiol*. 2019; 114:27.
<https://doi.org/10.1007/s00395-019-0735-0>
PMID:[31069509](https://pubmed.ncbi.nlm.nih.gov/31069509/)
41. Han D, Wang Y, Chen J, Zhang J, Yu P, Zhang R, Li S, Tao B, Wang Y, Qiu Y, Xu M, Gao E, Cao F. Activation of melatonin receptor 2 but not melatonin receptor 1 mediates melatonin-conferred cardioprotection against myocardial ischemia/reperfusion injury. *J Pineal Res*. 2019; 67:e12571.
<https://doi.org/10.1111/jpi.12571>
PMID:[30903623](https://pubmed.ncbi.nlm.nih.gov/30903623/)
42. Barbosa Lima LE, Muxel SM, Kinker GS, Carvalho-Sousa CE, da Silveira Cruz-Machado S, Markus RP, Fernandes PA. STAT1-NFκB crosstalk triggered by interferon gamma regulates noradrenaline-induced pineal hormonal production. *J Pineal Res*. 2019; 67:e12599.
<https://doi.org/10.1111/jpi.12599>
PMID:[31356684](https://pubmed.ncbi.nlm.nih.gov/31356684/)
43. Billah M, Ridiandries A, Rayner BS, Allahwala UK, Dona A, Khachigian LM, Bhindi R. Egr-1 functions as a master switch regulator of remote ischemic preconditioning-induced cardioprotection. *Basic Res Cardiol*. 2019; 115:3.
<https://doi.org/10.1007/s00395-019-0763-9>
PMID:[31823016](https://pubmed.ncbi.nlm.nih.gov/31823016/)
44. Thirugnanam K, Cossette SM, Lu Q, Chowdhury SR, Harmann LM, Gupta A, Spearman AD, Sonin DL, Bordas M, Kumar SN, Pan AY, Simpson PM, Strande JL, et al. Cardiomyocyte-Specific *Snrk* Prevents Inflammation in the Heart. *J Am Heart Assoc*. 2019; 8:e012792.
<https://doi.org/10.1161/JAHA.119.012792>
PMID:[31718444](https://pubmed.ncbi.nlm.nih.gov/31718444/)
45. Nowak-Sliwinska P, Alitalo K, Allen E, Anisimov A, Aplin AC, Auerbach R, Augustin HG, Bates DO, van Beijnum JR, Bender RH, Bergers G, Bikfalvi A, Bischoff J, et al. Consensus guidelines for the use and interpretation of angiogenesis assays. *Angiogenesis*. 2018; 21:425–532.
<https://doi.org/10.1007/s10456-018-9613-x>
PMID:[29766399](https://pubmed.ncbi.nlm.nih.gov/29766399/)
46. Yarana C, Thompson H, Chaiswing L, Butterfield DA, Weiss H, Bondada S, Alhakeem S, Sukati S, St Clair DK. Extracellular vesicle-mediated macrophage activation: an insight into the mechanism of thioredoxin-mediated immune activation. *Redox Biol*. 2019; 26:101237.
<https://doi.org/10.1016/j.redox.2019.101237>
PMID:[31276937](https://pubmed.ncbi.nlm.nih.gov/31276937/)
47. Herzog J, Schmidt FP, Hahad O, Mahmoudpour SH, Mangold AK, Garcia Andreo P, Prochaska J, Koeck T, Wild PS, Sørensen M, Daiber A, Münzel T. Acute exposure to nocturnal train noise induces endothelial dysfunction and pro-thromboinflammatory changes of the plasma proteome in healthy subjects. *Basic Res Cardiol*. 2019; 114:46.
<https://doi.org/10.1007/s00395-019-0753-y>
PMID:[31664594](https://pubmed.ncbi.nlm.nih.gov/31664594/)
48. Ding L, Gong C, Zhao J, Liu X, Li T, Rao S, Wang S, Liu Y, Peng S, Xiao W, Xiong C, Wang R, Liang S, Xu H. Noncoding transcribed ultraconserved region (T-UCR) UC.48+ is a novel regulator of high-fat diet induced myocardial ischemia/reperfusion injury. *J Cell Physiol*. 2019; 234:9849–61.
<https://doi.org/10.1002/jcp.27674>
PMID:[30417395](https://pubmed.ncbi.nlm.nih.gov/30417395/)
49. Qian W, Wang Z, Xu T, Li D. Anti-apoptotic effects and mechanisms of salvianolic acid A on cardiomyocytes in ischemia-reperfusion injury. *Histol Histopathol*. 2019; 34:223–31.
<https://doi.org/10.14670/HH-18-048> PMID:[30255492](https://pubmed.ncbi.nlm.nih.gov/30255492/)
50. Na HJ, Yeum CE, Kim HS, Lee J, Kim JY, Cho YS. TSPYL5-mediated inhibition of p53 promotes human endothelial cell function. *Angiogenesis*. 2019; 22: 281–93.
<https://doi.org/10.1007/s10456-018-9656-z>
PMID:[30471052](https://pubmed.ncbi.nlm.nih.gov/30471052/)
51. Zhang H, Jin B, Faber JE. Mouse models of Alzheimer's disease cause rarefaction of pial collaterals and increased severity of ischemic stroke. *Angiogenesis*. 2019; 22:263–79.
<https://doi.org/10.1007/s10456-018-9655-0>
PMID:[30519973](https://pubmed.ncbi.nlm.nih.gov/30519973/)
52. Zhu L, Wang J, Kong W, Huang J, Dong B, Huang Y, Xue W, Zhang J. LSD1 inhibition suppresses the growth of clear cell renal cell carcinoma *via* upregulating P21 signaling. *Acta Pharm Sin B*. 2019; 9:324–34.
<https://doi.org/10.1016/j.apsb.2018.10.006>
PMID:[30972280](https://pubmed.ncbi.nlm.nih.gov/30972280/)
53. Zhao J, Gao JL, Zhu JX, Zhu HB, Peng X, Jiang M, Fu Y, Xu J, Mao XH, Hu N, Ma MH, Dong DL. The different response of cardiomyocytes and cardiac fibroblasts to mitochondria inhibition and the underlying role of STAT3. *Basic Res Cardiol*. 2019; 114:12.

- <https://doi.org/10.1007/s00395-019-0721-6>
PMID:30767143
54. Zhu Y, Wang P, Zhang L, Bai G, Yang C, Wang Y, He J, Zhang Z, Zhu G, Zou D. Superhero Rictor promotes cellular differentiation of mouse embryonic stem cells. *Cell Death Differ.* 2019; 26:958–68.
<https://doi.org/10.1038/s41418-018-0177-5>
PMID:30154443
55. Zakeri Z, Lockshin RA, Diederich M. About canonical, non-canonical and immunogenic cell death: Basic mechanisms and translational applications: A meeting report of the International Cell Death Society. *Biochem Pharmacol.* 2019; 162:1–2.
<https://doi.org/10.1016/j.bcp.2018.09.011>
PMID:30222968
56. Zhang Z, Hu Q, Liu Y, Cheng P, Cheng H, Liu W, Xing X, Guan Z, Fang W, Chen S, Jiang J, Chen F. Strigolactone represses the synthesis of melatonin, thereby inducing floral transition in *Arabidopsis thaliana* in an FLC-dependent manner. *J Pineal Res.* 2019; 67:e12582.
<https://doi.org/10.1111/jpi.12582>
PMID:31012494
57. Zheng CJ, Yang LL, Liu J, Zhong L. JTC-801 exerts anti-proliferative effects in human osteosarcoma cells by inducing apoptosis. *J Recept Signal Transduct Res.* 2018; 38:133–40.
<https://doi.org/10.1080/10799893.2018.1436561>
PMID:29447541
58. Zheng HJ, Shen BB, Wang J, Wang H, Huo GL, Huang LR, Gao JQ, Fang WJ. Uncommon Peptide Bond Cleavage of Glucagon from a Specific Vendor under near Neutral to Basic Conditions. *Pharm Res.* 2019; 36:118.
<https://doi.org/10.1007/s11095-019-2647-y>
PMID:31161359
59. Shih YM, Cooke MS, Pan CH, Chao MR, Hu CW. Clinical relevance of guanine-derived urinary biomarkers of oxidative stress, determined by LC-MS/MS. *Redox Biol.* 2019; 20:556–65.
<https://doi.org/10.1016/j.redox.2018.11.016>
PMID:30508700
60. Zarfati M, Avivi I, Brenner B, Katz T, Aharon A. Extracellular vesicles of multiple myeloma cells utilize the proteasome inhibitor mechanism to moderate endothelial angiogenesis. *Angiogenesis.* 2019; 22:185–96.
<https://doi.org/10.1007/s10456-018-9649-y>
PMID:30386953
61. Zulato E, Ciccarese F, Agnusdei V, Pinazza M, Nardo G, Iorio E, Curtarello M, Silic-Benussi M, Rossi E, Venturoli C, Panieri E, Santoro MM, Di Paolo V, et al. LKB1 loss is associated with glutathione deficiency under oxidative stress and sensitivity of cancer cells to cytotoxic drugs and γ -irradiation. *Biochem Pharmacol.* 2018; 156:479–90.
<https://doi.org/10.1016/j.bcp.2018.09.019>
PMID:30222967
62. Man S, Sanchez Duffhues G, Ten Dijke P, Baker D. The therapeutic potential of targeting the endothelial-to-mesenchymal transition. *Angiogenesis.* 2019; 22:3–13.
<https://doi.org/10.1007/s10456-018-9639-0>
PMID:30076548
63. Zhang Y, Zou X, Qian W, Weng X, Zhang L, Zhang L, Wang S, Cao X, Ma L, Wei G, Wu Y, Hou Z. Enhanced PAPSS2/VCAN sulfation axis is essential for Snail-mediated breast cancer cell migration and metastasis. *Cell Death Differ.* 2019; 26:565–79.
<https://doi.org/10.1038/s41418-018-0147-y>
PMID:29955124
64. Zientara A, Stephan M, von Hörsten S, Schmiedl A. Differential severity of LPS-induced lung injury in CD26/DPP4 positive and deficient F344 rats. *Histol Histopathol.* 2019; 34:1151–71.
<https://doi.org/10.14670/HH-18-117>
PMID:30977110
65. Lan YL, Zou YJ, Lou JC, Xing JS, Wang X, Zou S, Ma BB, Ding Y, Zhang B. The sodium pump $\alpha 1$ subunit regulates bufalin sensitivity of human glioblastoma cells through the p53 signaling pathway. *Cell Biol Toxicol.* 2019; 35:521–39.
<https://doi.org/10.1007/s10565-019-09462-y>
PMID:30739221
66. Álvarez-Fernández M, Sanz-Flores M, Sanz-Castillo B, Salazar-Roa M, Partida D, Zapatero-Solana E, Ali HR, Manchado E, Lowe S, VanArsdale T, Shields D, Caldas C, Quintela-Fandino M, Malumbres M. Therapeutic relevance of the PP2A-B55 inhibitory kinase MASTL/Greatwall in breast cancer. *Cell Death Differ.* 2018; 25:828–40.
<https://doi.org/10.1038/s41418-017-0024-0>
PMID:29229993
67. Balduini W, Weiss MD, Carloni S, Rocchi M, Sura L, Rossignol C, Longini M, Bazzini F, Perrone S, Ott D, Wadhawan R, Buonocore G. Melatonin pharmacokinetics and dose extrapolation after enteral infusion in neonates subjected to hypothermia. *J Pineal Res.* 2019; 66:e12565.
<https://doi.org/10.1111/jpi.12565> PMID:30734962
68. Dong P, Hao F, Dai S, Tian L. Combination therapy Eve and Pac to induce apoptosis in cervical cancer cells by targeting PI3K/AKT/mTOR pathways. *J Recept Signal Transduct Res.* 2018; 38:83–88.
<https://doi.org/10.1080/10799893.2018.1426610>
PMID:29369007